PERGAMON

International Journal of Heat and Mass Transfer 45 (2002) 145–156

International Journal of HEAT and MASS TRANSFER

www.elsevier.com/locate/ijhmt

Flow visualization and film cooling effectiveness measurements around shaped holes with compound angle orientations

Hong-Wook Lee, Jung Joon Park, Joon Sik Lee *

Institute of Advanced Machinery and Design, School of Mechanical and Aerospace Engineering, Seoul National University, Seoul 151-742, Republic of Korea

Received 28 June 2000; received in revised form 5 January 2001

Abstract

Experimental results are presented which describe film cooling performance around shaped holes with compound angle orientations. The shaped hole has a 15° forward expansion with an inclination angle of 35°, but the orientation angles vary from 0° to 30° and 60°. The blowing ratios considered are 0.5, 1.0 and 2.0. Flow visualizations are performed using an aerosol seeding method for single enlarged shaped hole to investigate the interaction between the mainstream and the injectant at the hole exit plane. The adiabatic film cooling effectiveness distributions are measured for a single row of seven shaped holes using the thermochromic liquid crystal technique. Flow visualization reveals the occurrence of hot crossflow ingestion into the film hole at the hole exit plane at a large orientation angle such as 60°. Shaped holes with simple angle injection do not provide substantial improvement in the film cooling performance compared to round holes. However, shaped holes with compound angle injection exhibit improved film cooling effectiveness up to 55% in comparison with round hole data at high blowing ratios. © 2001 Published by Elsevier Science Ltd.

1. Introduction

Discrete hole film cooling is an effective cooling technique applied to gas turbine blades. Most of previous researchers on discrete hole film cooling have concentrated on simple round holes. Although it has been over 25 years since Goldstein et al. [1] first reported the exceptional film cooling performance of shaped cooling holes, transferring the laboratory configuration to practical turbine was seriously limited by the difficulties in manufacturability, durability, maintenance, etc. However, nowadays people are getting more interested in film cooling with shaped holes because improvements in manufacturing techniques and development of new materials make it possible to adopt shaped film cooling holes in real turbine blades.

Among earliest studies, Goldstein et al. [1] used a 35°-inclined axial injection hole with an initially round cross-section widened to each side by 10°. They reported a significant increase in the film cooling effectiveness in the near hole region as well as an improved lateral spread of the coolant. Makki and Jakubowski [2] presented downstream heat transfer results for film holes that had trapezoidal cross-sections and were diffused in the direction of the mainstream flow. Their experimental data showed that the trapezoidal shaped holes offer up to 23% better film cooling performance than the corresponding round holes. Schmidt et al. [3] and Sen et al. [4] examined the performance of forward-expanded holes with compound angle orientation. They showed that the film-cooling performance with expanded holes is improved in the case of large momentum flux ratios. In the measurement of flow field with injection from expanded holes, Thole et al. [5] found that by expanding the exits of the cooling holes, the penetration of the injectant into the mainstream boundary layer and the intense shear regions are significantly reduced compared to the round hole injection. McGrath and Leylek [6] conducted numerical simulations for the same hole configuration of Schmidt et al. [3] and Sen et al. [4]. They reported that the forward expanded hole provides substantial

* Corresponding author.

0017-9310/02/$ - see front matter © 2001 Published by Elsevier Science Ltd.
PII: S0017-9310(01)00112-0

Nomenclature

D	film cooling hole diameter
DR	density ratio ($=\rho_c/\rho_\infty$)
H	shape factor ($=\delta^*/\theta$)
I	momentum flux ratio of coolant to mainstream ($=\rho_c U_c^2/\rho_\infty U_\infty^2$)
L	film cooling hole length
M	blowing ratio ($=\rho_c U_c/\rho_\infty U_\infty$)
Re_D	Reynolds number based on film cooling hole diameter ($=U_\infty D/\nu$)
T	temperature
U	velocity
x	streamwise coordinate originating at the trailing edge of cooling holes
z	spanwise coordinate originating at the trailing edge of the central cooling hole

Greek symbols

β	orientation angle of the cooling hole
δ	boundary layer thickness
δ^*	displacement thickness
η	local adiabatic film cooling effectiveness ($=(T_{aw}-T_\infty)/(T_c-T_\infty)$)
$\bar{\eta}$	spanwise-averaged adiabatic film cooling effectiveness
$\overline{\overline{\eta}}$	space-averaged adiabatic film cooling effectiveness
θ	momentum thickness
ρ	density
ν	kinematic viscosity

Subscripts

aw	adiabatic wall
c	coolant
r	round hole
s	shaped hole
∞	mainstream

improvement in the film cooling performance, however, simultaneously producing undesirable crossflow ingestion into the film hole, which might cause a severe thermal failure.

More recently, Cho et al. [7] investigated the effects of compound angle on film cooling performance of a single conical-shaped hole. The adopted orientation angles were 0°, 45° and 90°. Their results indicated that the injected jet protects the surface effectively with low blowing rates and spreads more widely with the compound angle injections than the axial injection. Reiss and Bölcs [8] reported that the laid-back shaped holes applied to leading edge film cooling lead to a clear enhancement of the cooling performance compared to round holes, whereas laterally expanded holes give only slight performance enhancement. Kohli and Bogard [9] examined the shaped holes with the large injection angle of 55°. Although performance degraded with increase of the injection angle, shaped holes with large angle injection showed better cooling performance than round holes with the standard 35° angle injection.

Although many researchers have reported that shaped holes have a prominent cooling performance, there has been no experimental study that can verify previous numerical finding, "hot crossflow ingestion", and there are only few of studies on the effects of compound angle with shaped holes.

This paper presents adiabatic effectiveness data and flow visualization for shaped holes with compound angle orientations. The holes adopted in this study have a 15° forward expansion with an inclination angle of 35° and orientation angles of 0°, 30° and 60°. The blowing ratio varies from 0.5 to 2.0. The interaction between the mainstream and the injectant is visualized using single enlarged shaped hole at the hole exit plane. Flow visualization focuses on crossflow ingestion into the hole. The film cooling effectiveness distributions are measured for a row of seven shaped holes using the thermochromic liquid crystal technique. Detailed effectiveness distributions show clearly the effect of compound angle on the film cooling performance of shaped hole.

2. Experimental apparatus and procedure

A schematic of the wind tunnel and the injectant supply system is shown in Fig. 1. The wind tunnel is an open-circuit and subsonic, with a 6.25–1 contraction ratio nozzle. The test section is 400 mm wide, 280 mm high, and 3360 mm long. At a free-stream velocity of 10 m/s, flow at the test section inlet shows excellent spatial uniformity with spanwise velocity variation less than 0.3%, and a turbulence level less than 0.3%. A boundary layer trip wire of 2.4 mm in diameter is located on the test plate just downstream of the nozzle exit. The air, used as the injectant, first flows through an orifice followed by two heat exchangers that control the injectant temperature. The air is then ducted to a plenum chamber and discharged through the injection holes.

The geometry of shaped film cooling holes and the coordinate system are shown in Fig. 2. The origin of the coordinate system is located at the trailing edge (TE) of the central hole. The film cooling holes have a 15° forward expansion with an inclination angle of 35°, which

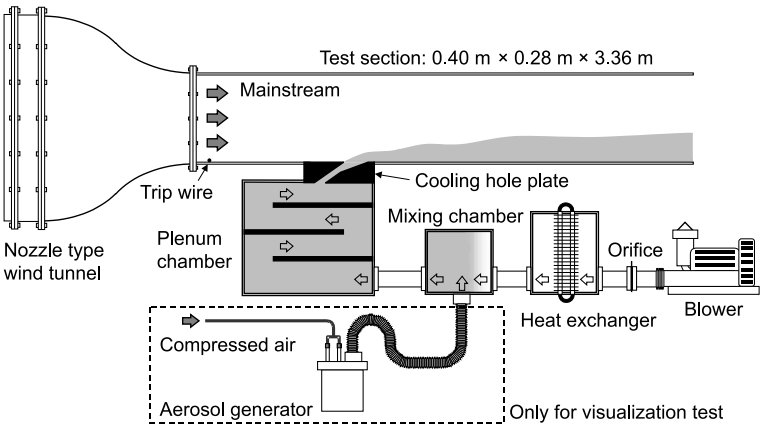

Fig. 1. Schematic view of the film cooling test facility.

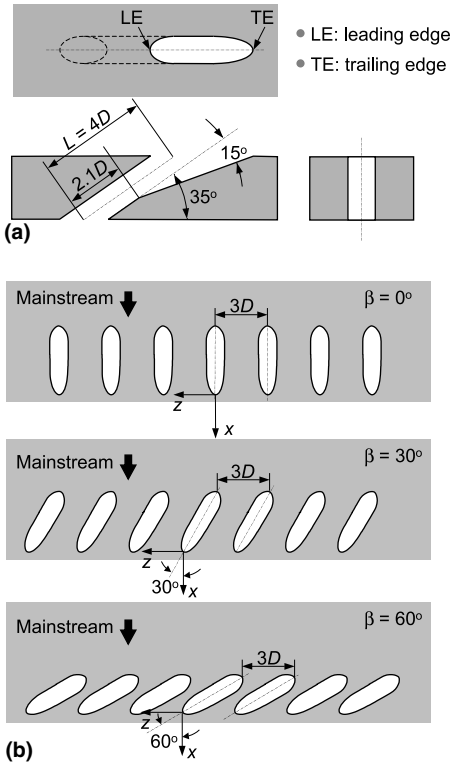

Fig. 2. Shaped hole geometry and orientation angle: (a) hole geometry; (b) orientation angle and coordinate system.

are exact replicas of previous studies [3,4,6]. The film hole plates are prepared for each orientation angle of 0°, 30° and 60°. The inclination angle is defined as the angle between the injection vector and its projection on the x–z plane, whereas the orientation angle is defined as the angle between the streamwise direction and the projection of the injection vector on the x–z plane. Experimental conditions at the leading edge (LE) of the film cooling hole are listed in Table 1.

Table 1
Experimental conditions

	Visualization	Effectiveness
U_∞ (m/s)	10	10
D (mm)	30 (single hole)	15 (single row)
Re_D	19 200	9 600
δ/D	0.8	1.6
δ^*/D	0.11	0.21
θ/D	0.08	0.15
H	1.4	1.4
β	0°, 30°, 60°	0°, 30°, 60°
M	0.5, 1.0, 1.5, 2.0	0.5, 1.0, 2.0

2.1. Flow visualization

The aerosol seeding method is used for the present flow visualization. Fig. 3(a) shows the experimental set-up for the visualization test. In all cases, single shaped hole with a diameter of 30 mm is used. The leading edge of the injection hole is located at 750 mm downstream from the trip wire. Two sets of 20 mW He–Ne laser and cylindrical lens are used to get a thin laser sheet. This laser sheet is positioned parallel to and 1 mm above the film cooled surface. Oil aerosols produced by an aerosol generator of Echols and Young [10] are mixed with the injectant in a mixing chamber. The cross-section of the injectant trajectory at the hole exit plane is illuminated by the laser sheet, and the injectant motions are captured by a high speed camera (Kodak, SR-Ultra), which is aligned perpendicular to the test surface. The captured images are downloaded as standard TIFF files via the SCSI-2 port directly to a personal computer. Image-processing steps for averaging and image correction are then performed.

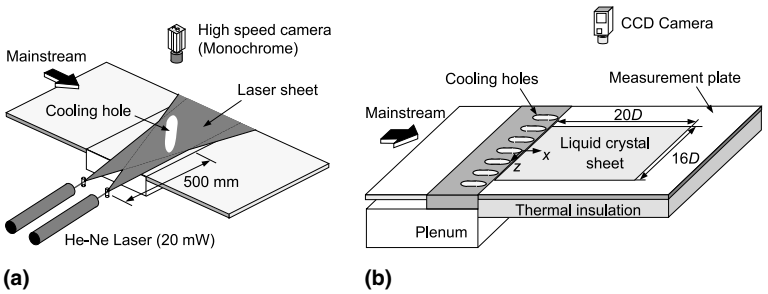

Fig. 3. Experimental set-up for visualization and film cooling effectiveness measurement: (a) visualization; (b) film cooling effectiveness measurement.

2.2. Adiabatic film cooling effectiveness

The adiabatic film cooling effectiveness, which indicates the measure of film coverage, is defined as

$$\eta = \frac{T_{aw} - T_\infty}{T_c - T_\infty}, \tag{1}$$

where T_{aw}, T_∞ and T_c are the adiabatic wall temperature, the mainstream temperature and the injectant temperature, respectively. The adiabatic film cooling effectiveness can thus be obtained from the adiabatic wall temperature measurement.

For the film cooling effectiveness measurements, a row of seven holes with a diameter of 15 mm is used. The trailing edge of the hole is located 51D downstream of the trip wire. The hole spacing between the hole centers is 3D. As described in Fig. 3(b), the test section consists of a film hole plate and a measurement plate. To measure the temperature distribution on the entire test surface downstream of the injection holes, a thermochromic liquid crystal (TLC) sheet is used. The TLC sheet covers the test plate in the range of $0.4 \leqslant x/D \leqslant 20.4$ and $-8.0 \leqslant z/D \leqslant 8.0$. The TLC sheet is attached just on a 12.4 mm thick polycarbonate plate. A foamed polystyrene sheet of 50 mm thick is used for insulation. A CCD camera is used to capture TLC color images, which is aligned perpendicular to the TLC sheet 1200 mm away. Two 150 W Halogen lamps, which are used as light source, are positioned at an angle of 35° with the TLC sheet 1 100 mm away. The TLC sheet is illuminated only when the capturing is in progress to prevent radiation heating from the illuminators.

Among many techniques, the steady-state hue capturing method [11–13] is adopted in this study. The liquid crystal used to measure effectiveness distributions has a color changing temperature range from 20°C to 30°C. Since the bandwidth of the TLC sheet is wide enough, the sheet can map the entire isothermal pattern of the surface from a single image. When temperature is measured with the TLC, extra care is taken to set all the conditions identical with the calibration conditions to avoid the color variation problem. The relationship between the hue value of the color image and temperature is obtained in the form of a polynomial curve fit. The curve coefficients are used to find the surface temperature from the measured image.

The mainstream and the injectant temperatures are measured by thermocouples that are calibrated in a constant thermal bath with a precision platinum resistance thermometer.

The uncertainty analysis is evaluated on 20 to 1 odds (95 percent confidence level). All the uncertainty values are evaluated from the method of single-sample experiments proposed by Kline and McClintock [14]. The uncertainty of the adiabatic film cooling effectiveness is ± 0.014 at a η value of 0.2. The uncertainty value is slightly large at the low effectiveness value. For example, the uncertainty value is ± 0.013 at $\eta = 0.5$ but ± 0.015 at $\eta = 0.05$.

3. Results and discussion

3.1. Flow visualization

Fig. 4(a)–(c) show the flow visualization images at $\beta = 60°$ which are captured instantaneously with exposing time of 1/60 s. The dark image in the hole indicates mainstream flow across the exit plane. Fig. 4(d)–(f) show contours of the normalized vertical velocity component at the hole exit plane, which are numerical simulation results of McGrath and Leylek [6]. These figures clearly show excellent agreement between visualization and numerical simulation.

In the case of $M = 0.5$, mainstream penetrates into the injectant region in a saw-toothed pattern along the upstream edge of the hole exit plane (Fig. 4(a)). The saw-toothed image is similar to contour line value of 0.1 in Fig. 4(d). As the injectant has relatively low momentum at $M = 0.5$, mainstream penetrates into the injectant along the most part of the upstream edge of the hole exit plane.

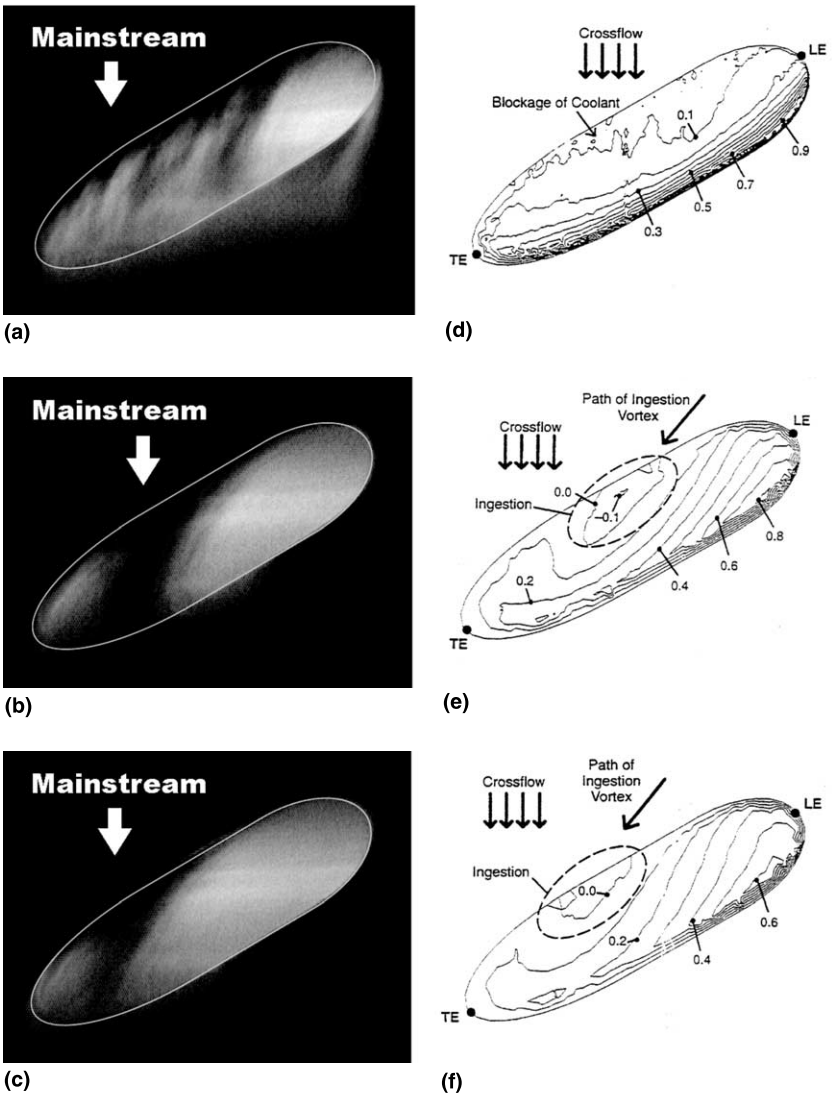

Fig. 4. Flow visualization at $\beta = 60°$ in comparison with numerical analysis [6]: (a) $M = 0.5, I = 0.25$; (b) $M = 1.0, I = 1.00$; (c) $M = 1.5, I = 2.25$; (d) $M = 0.5, I = 0.13$; (e) $M = 1.25, I = 0.98$; (f) $M = 1.88, I = 2.21$.

Visualizations at $M = 1.0$ and 1.5 show that the mainstream flows across the hole exit plane near the trailing edge. This flow behavior results from the geometric peculiarity of the hole. The injectant coming out from the trailing edge side of the film hole slows down near the exit because the trailing edge is made of a diffusion section (expanded trailing edge), while the injectant from the leading edge side retains its momentum. Mainstream thus flows across the hole exit plane near the trailing edge where the injectant momentum is relatively low. This result supports "hot crossflow ingestion" which is predicted by the numerical simulation [6]. As shown in Fig. 4(e) and (f), in the region where the normalized velocities are negative, mainstream fluid flows into the injection hole, which might cause severe thermal failure of the blade.

Fig. 5 shows time-averaged images over 500 instantaneous captures. At $M = 0.5$, the injectant spreads laterally well around the hole for all orientation angles, which could provide good film cooling performance. As the blowing ratio increases, lateral spreading of the injectant is not observed near the hole. The orientation angle of the shaped holes also affects the interaction between the injectant and the mainstream. As previously shown in Fig. 4, there is a significant penetration of the mainstream into the injectant at $\beta = 60°$. At $\beta = 30°$, this flow ingestion is not significant but is still observed along the upstream edge of the hole at $M = 0.5$. When

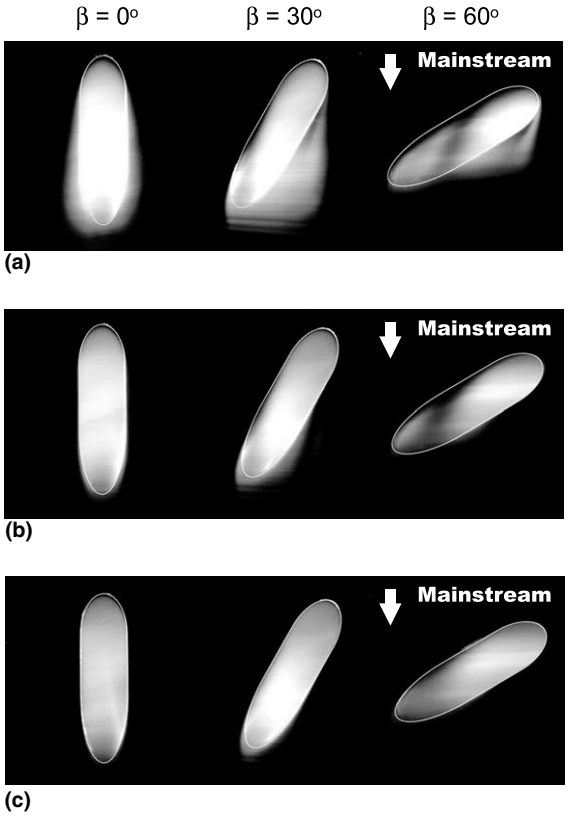

Fig. 5. Time-averaged images of injectant behavior: (a) $M = 0.5$; (b) $M = 1.0$; (c) $M = 2.0$.

$\beta = 0°$, the injectant is not affected by the mainstream except at the leading edge.

3.2. Adiabatic film cooling effectiveness

Figs. 6–8 show the adiabatic film cooling effectiveness distributions at $M = 0.5$, 1.0 and 2.0, respectively. As expected from flow visualization, the adiabatic effectiveness in the near hole region is higher at $M = 0.5$ than at other blowing ratios. In the case of $\beta = 0°$, the effectiveness shows symmetric distribution with respect to the hole centerline, and effectiveness values are much higher along the hole centerlines than in the region between the holes. As the orientation angle increases, however, the lateral variation of the effectiveness is smoothed and becomes more uniform at $\beta = 60°$. This is simply because the strength of the lateral component of the injectant momentum increases with compound angle and hence the injectant spreads in the spanwise direction to cover the region between the holes. This is evidenced by the fact that local peaks in the effectiveness contour shifted toward z-direction as the orientation angle increases.

An interesting fact to note is that in Fig. 6(c), two high peak points in the effectiveness distribution are observed immediately downstream of hole. This results from mainstream penetration into the injectant at the hole exit plane as described earlier. Detailed description is presented in Fig. 9. As shown in Fig. 9(a), the mainstream fluid flows into the hole across the hole center

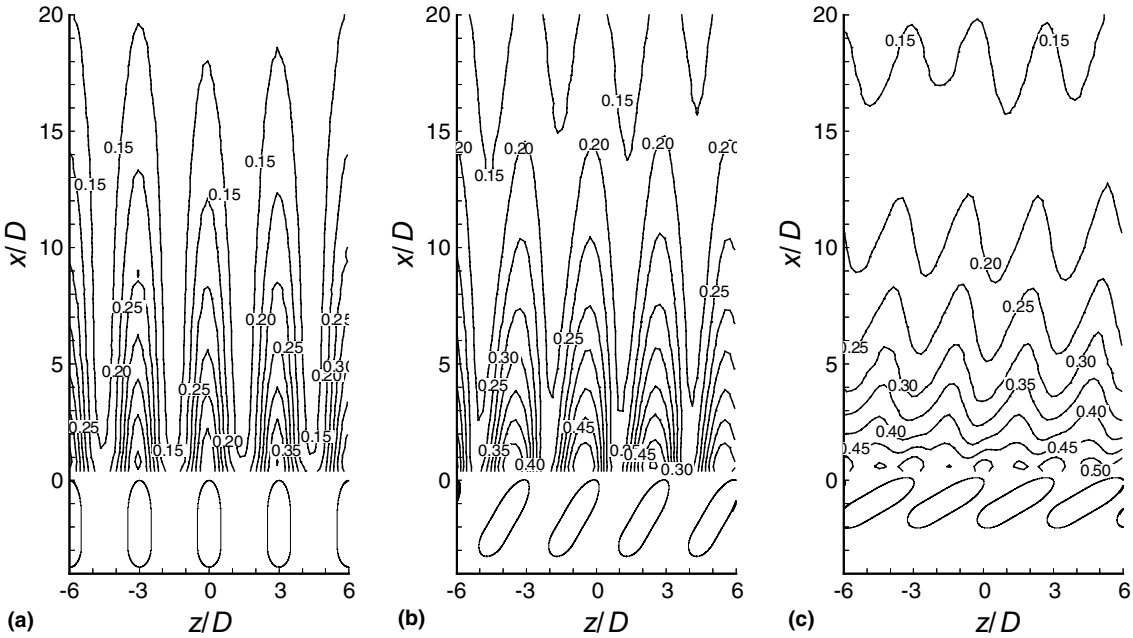

Fig. 6. Adiabatic film cooling effectiveness distributions at $M = 0.5$: (a) $\beta = 0°$; (b) $\beta = 30°$; (c) $\beta = 60°$.

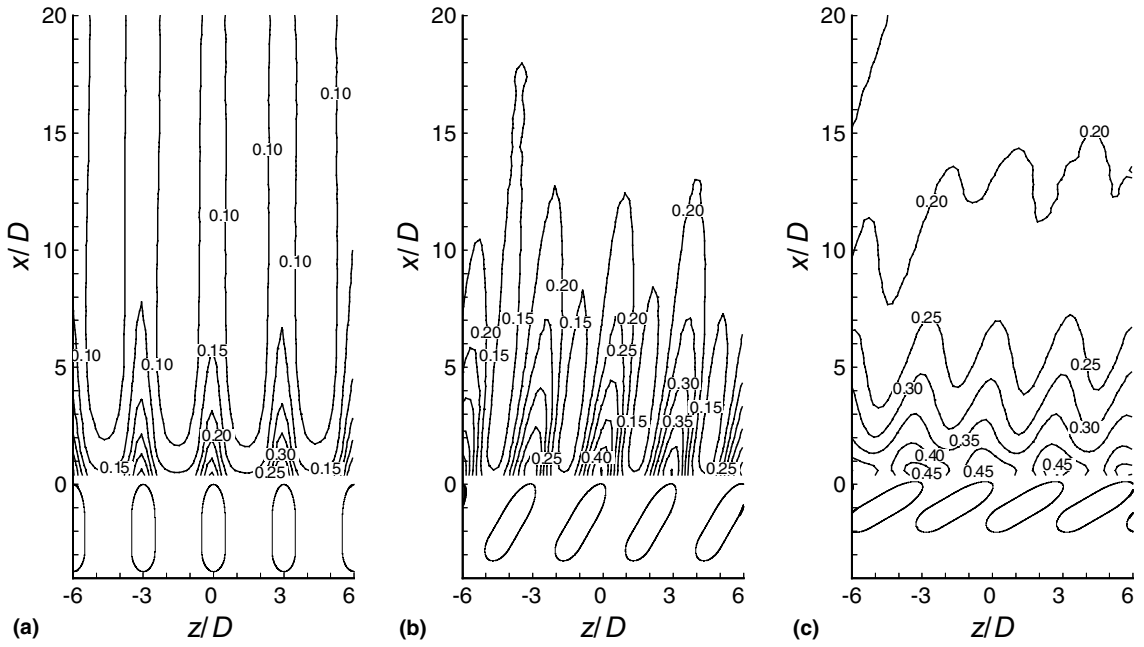

Fig. 7. Adiabatic film cooling effectiveness distributions at $M = 1.0$: (a) $\beta = 0°$; (b) $\beta = 30°$; (c) $\beta = 60°$.

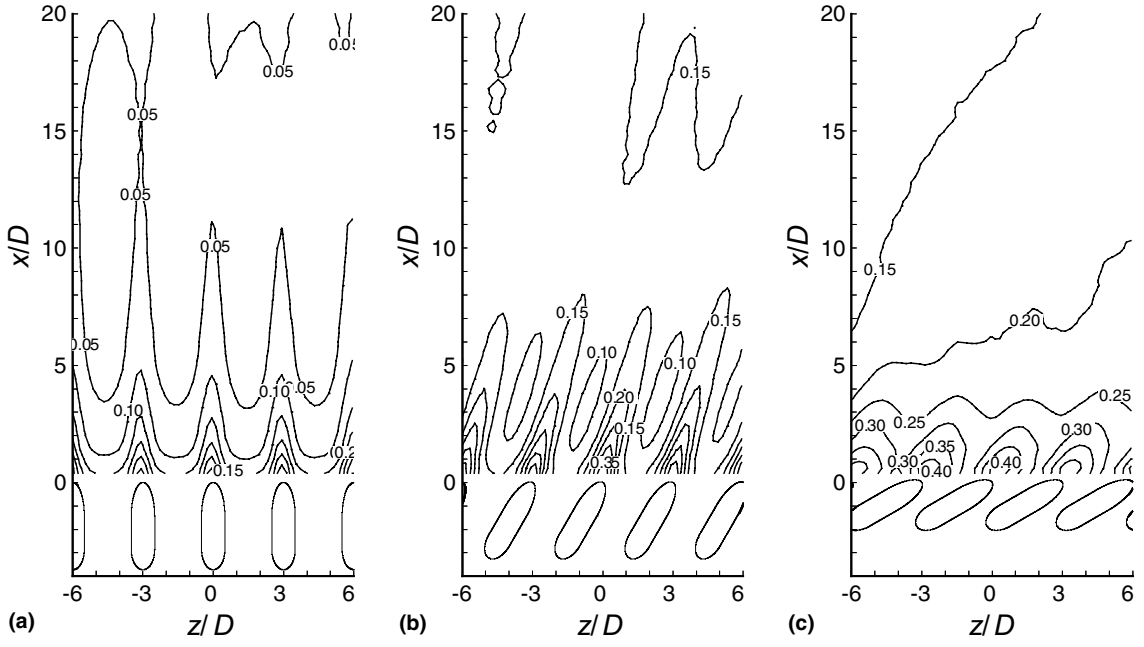

Fig. 8. Adiabatic film cooling effectiveness distributions at $M = 2.0$: (a) $\beta = 0°$; (b) $\beta = 30°$; (c) $\beta = 60°$.

region, which blocks the injectant flow there and separates the injectant into two streams. The spanwise effectiveness distribution at $x/D = 1.0$ shown in Fig. 10(a) clearly reflects this flow behavior. The first high peak at about $z/D = 3.0$ is due to the injectant coming out from the trailing edge side of the hole, the low peak next to this point (at about $z/D = 2.4$) is due to the ingestion of the mainstream fluid which results in low injectant

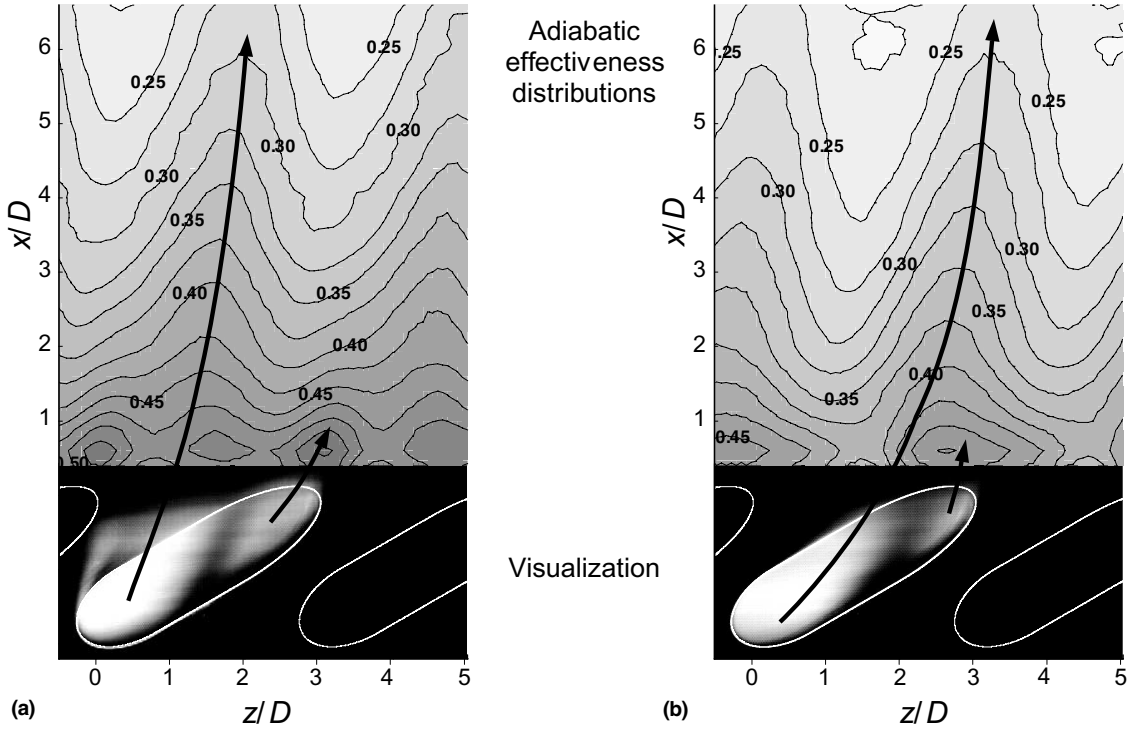

Fig. 9. Relation of adiabatic effectiveness distributions with injectant behaviors at $\beta = 60°$: (a) $M = 0.5$; (b) $M = 1.0$.

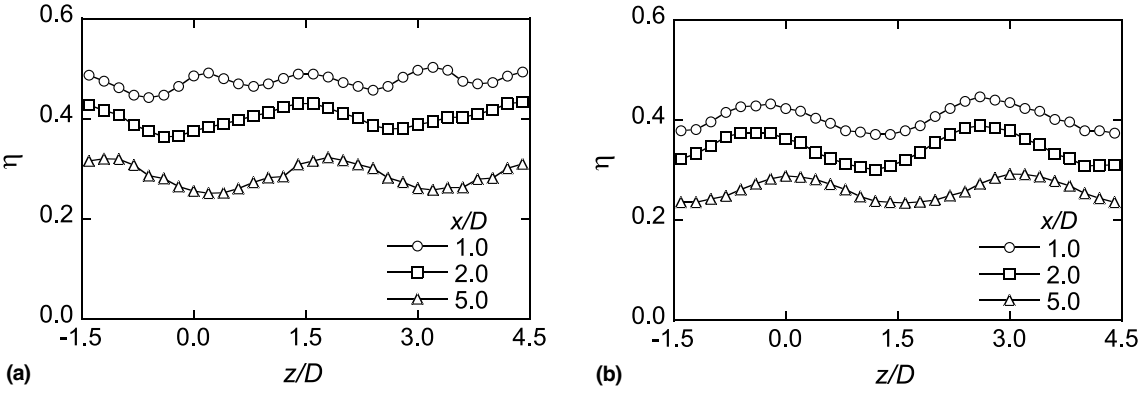

Fig. 10. Spanwise adiabatic effectiveness distributions at $\beta = 60°$: (a) $M = 0.5$; (b) $M = 1.0$.

concentration by mixing, and the second high peak at about $z/D = 1.5$ is due to the injectant from the leading edge side of the adjacent hole. Beyond $x/D = 1.0$, the first high peak disappears due to the mixing of the injectant with mainstream fluid as moving downstream, and only the second high peak is observed. This is because a larger portion of the coolant is injected through the leading edge side of the hole, and a smaller portion from the trailing edge side is swept way by the mainstream immediate downstream of the hole exit. At $M = 1.0$, however, as almost all of the trailing edge side of the hole is blocked by the mainstream (Fig. 9(b)), such a high peak between the holes does not exist (Fig. 10(b)).

As the blowing ratio increases to 1.0, the effectiveness values decrease as shown in Fig. 7 because the injectant trajectory lifts slightly off from the wall due to the increasing vertical momentum of the injectant. In compound angle injection, however, the effectiveness is relatively high and uniform compared to simple angle

injection ($\beta = 0°$). Since with compound angle orientation ($\beta = 30°$ and $60°$), the injectant has both vertical and lateral components of momentum, the magnitude of the vertical momentum is smaller than that with simple angle injection. Thus, the injectant is well attached and spreads over the wall to yield higher effectiveness values.

Fig. 8 shows the effectiveness distributions at the blowing ratio of 2.0. As the blowing ratio increases to 2.0, the effectiveness decreases so that the downstream surface is practically unprotected by the injectant. At $\beta = 60°$, however, the relatively high and uniform effectiveness values are maintained over the entire measured surface including the region between holes.

The round hole results of Jung and Lee [15] are used as the baseline data to investigate the effect of hole shaping. They measured the effectiveness distributions of round holes with compound angle using the same experimental facilities as the present study. To verify their results as baseline data, the effectiveness distributions are compared with the results from Schmidt et al. [3], who conducted experimental study for round hole and forward expanded hole. Fig. 11 shows the streamwise variation of spanwise-averaged effectiveness ($\bar{\eta}$) at the blowing ratio of 0.5. The spanwise-averaged effectiveness distributions of Schmidt et al. [3] are larger than that from Jung and Lee [15] and the present study with nearly a constant difference. However, the effectiveness distribution of Goldstein et al. [16], who measured film cooling effectiveness distribution using naphthalene sublimation technique ($DR = 1.0$), shows good agreement with that of Jung and Lee [15]. The difference with results of Schmidt et al. [3] is primarily attributed to the differences in density ratio of injectant to mainstream. The density ratio, DR, is 1.6 in the work of Schmidt et al. [3], while DR in the Jung and Lee [15]'s work and the present study is 0.93. If the effect of density ratio is taken into consideration, the round hole data of Jung and Lee [15] and the shaped hole data of present study both show fairly good agreement with the results of Schmidt et al. [3]. Therefore, there seems to be no significant problem in adopting Jung and Lee [15]'s results as the baseline data.

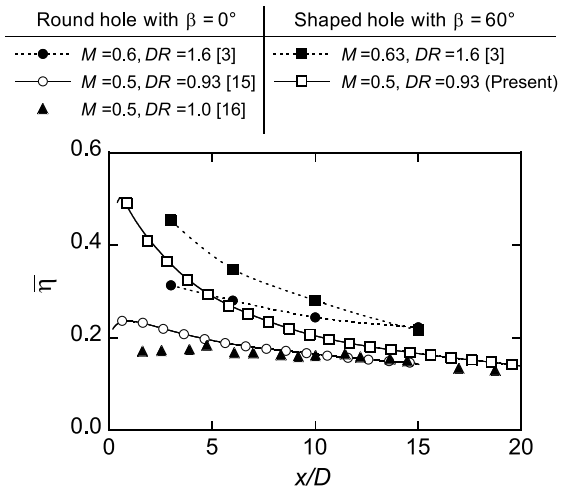

Fig. 11. Comparison of spanwise-averaged effectiveness to published data.

The streamwise variation of the spanwise-averaged adiabatic film cooling effectiveness, $\bar{\eta}$, is presented in Fig. 12 in comparison with round hole data of Jung and Lee [15] for three different blowing ratios. The shaped hole film cooling is, in general, more effective than the round hole film cooling especially at the larger orientation angles and blowing ratios, and the effectiveness values are higher at the larger orientation angles. As the blowing ratio increases, the effectiveness values decrease, especially in the near hole region. For example, when $\beta = 60°$, the effectiveness value at the immediate hole exit decreases from $\bar{\eta} = 0.50$–0.35 (30% reduction) as the blowing ratio increases from 0.5 to 2.0. However, in the downstream region where $x/D = 20$, $\bar{\eta}$ value is about the same as 0.15 regardless of the blowing ratio. This implies the decrease rate in the streamwise direction is higher at the lower blowing ratio.

When $M = 0.5$, compared to the round hole data, the shaped holes provide higher effectiveness values near the hole, but in the downstream region for $x/D > 10$, no difference is observed between two hole shapes regardless of orientation angle. This is because the injectant from round holes is also attached well to the wall at the low blowing ratio.

At $M = 1.0$ the shaped hole effectiveness values are larger than the round hole effectiveness values in the entire measurement range except those with simple angle injection ($\beta = 0°$). Another fact is that the shaped hole effectiveness decreases quite rapidly in the streamwise direction while the round hole effectiveness distribution remains almost uniform. When $M = 2.0$, the round hole effectiveness shows strikingly different variation in the streamwise direction in such a way that the effectiveness increases from a certain point in the downstream region. This is caused due to the reattachment of the injectant trajectory after lifting off from the wall immediate downstream of the hole exit at higher blowing ratios. In contrast to the round hole effectiveness distributions, the shaped hole effectiveness variation in the streamwise direction is very similar to that at $M = 1.0$ except a little reduction in the magnitude of the effectiveness value. Thus, it can be presumed that with shaped hole injection, the injectant spreads over the surface without lifting off even at a high blowing ratio such as $M = 2.0$ because of the expanded trailing edge of the hole.

The shaped hole with simple angle injection ($\beta = 0°$) does not show much improvement in the effectiveness

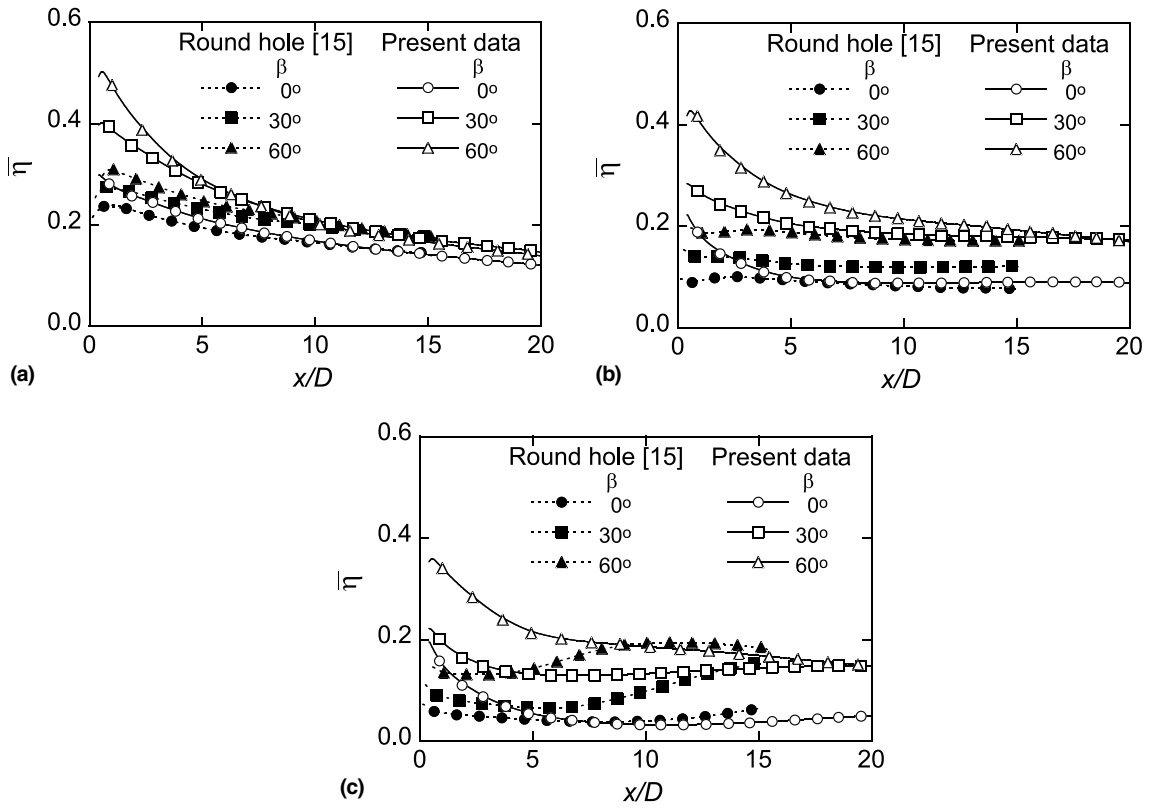

Fig. 12. Streamwise variation of spanwise-averaged adiabatic film cooling effectiveness: (a) $M = 0.5$; (b) $M = 1.0$; (c) $M = 2.0$.

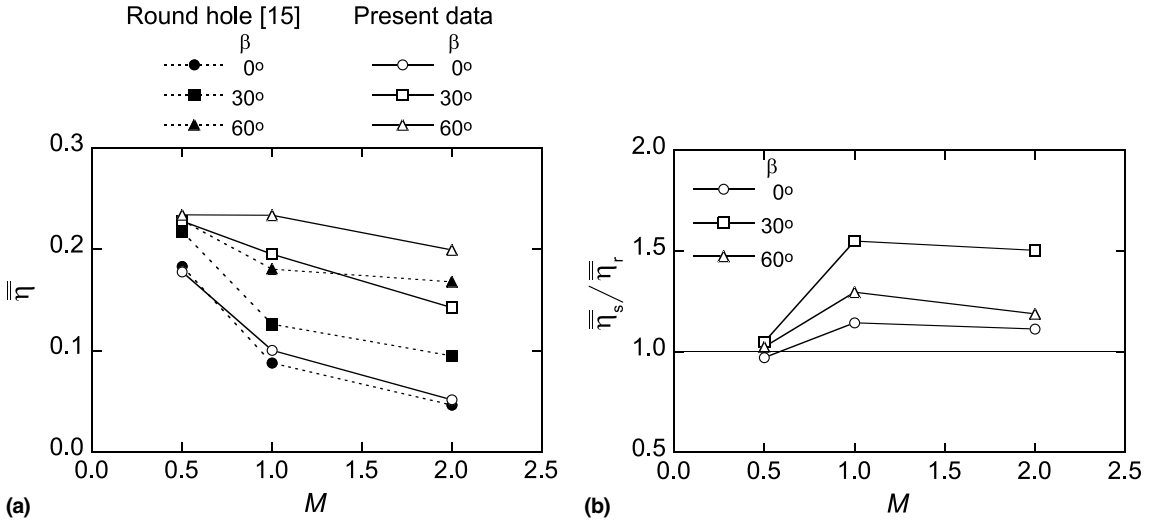

Fig. 13. Space-averaged adiabatic film cooling effectiveness: (a) with respect to orientation angle; (b) normalized with round hole data.

especially for $x/D > 5$ compared to the round hole for all blowing ratios. On the other hand, the shaped hole with compound angle injection exhibits a notable improvement in the effectiveness.

To compare the effectiveness over a full range of blowing ratios and orientation angles, the space-averaged adiabatic effectiveness, $\overline{\overline{\eta}}$, is used. For comparison with the reference data, this quantity is defined as the

integral average of the spanwise-averaged effectiveness from $x/D = 0.6$ to 15.6. Fig. 13(a) shows the resulting values of $\overline{\overline{\eta}}$ for the three orientation angles as a function of blowing ratio in comparison with round hole [15]. An observation stands out that regardless of hole shape, compound angle injection holes have the similar space-averaged effectiveness value of about 0.22 at $M = 0.5$, while those of simple angle injection hole are relatively low values of about 0.18. It can be deduced that at the low blowing ratio, a significant improvement in effectiveness can be achieved with only a slight change of orientation angle for both round hole and the current forward expanded hole. As the blowing ratio increases, the space-averaged effectiveness values for the shaped hole as well as the round hole monotonously decrease. However, the space-averaged effectiveness values for the shaped hole with $\beta = 60°$ decrease only slightly, and are essentially the same over the full range of the blowing ratio tested. It can be stated that the compound angle of the forward expanded hole becomes more effective at high blowing ratios.

The space-averaged effectiveness for the shaped holes ($\overline{\overline{\eta}}_s$) is normalized with that for round hole ($\overline{\overline{\eta}}_r$) in Fig. 13(b). From the normalized effectiveness values ($\overline{\overline{\eta}}_s/\overline{\overline{\eta}}_r$), it is obvious that the effect of forward expansion in hole geometry is negligible at a low blowing ratio, where the forward expanded hole with simple angle injection shows similar performance with round hole. On the other hand, at high blowing ratios, shaped holes show improved effectiveness values for all orientation angles in comparison with round holes. Although shaped holes with 60° compound angle injection have the highest effectiveness values for all blowing ratios, the forward expanded hole with 30° compound angle injection shows the most improvement in film cooling effectiveness of up to 55% in comparison with round hole.

4. Conclusions

Flow visualization and film cooling effectiveness measurement have been conducted using shaped holes with compound angle orientations. Shaped holes have a 15° forward expansion with a fixed inclination angle of 35°. The orientation angles of 0°, 30° and 60°, and the blowing ratios of 0.5, 1.0 and 2.0 are investigated. Flow in the injectant exit plane is visualized using oil aerosol particles, and the adiabatic film cooling effectiveness is measured using the thermochromic liquid crystal technique. Some important observations are noticed and summarized below.

1. Flow visualization shows occurrence of reverse flow from mainstream to the film hole at the hole exit plane when $\beta = 60°$, which supports previous numerical finding, ''hot crossflow ingestion''.
2. The lateral spreading of the injectant around the shaped hole is observed even at the high blowing ratio, which results in a great improvement in the adiabatic film cooling effectiveness.
3. Shaped holes with simple angle orientations do not provide substantial improvement in the film cooling performance compared to round holes. However, the shaped holes exhibit a notable improvement with compound angle injection. Thus, it is recommended that the forward expanded hole be adopted in combination with compound angle orientations.

References

[1] R.J. Goldstein, E.R.G. Eckert, F. Burggraf, Effects of hole geometry and density on three-dimensional film cooling, Int. J. Heat Mass Transfer 17 (1974) 595–607.
[2] Y.H. Makki, G.S. Jakubowski, An experimental study of film cooling from diffused trapezoidal shaped holes, AIAA Paper No. 86-1326, 1986.
[3] D.L. Schmidt, B. Sen, D.G. Bogard, Film cooling with compound angle holes: adiabatic effectiveness, ASME J. Turbomachinery 118 (1996) 807–813.
[4] B. Sen, D.L. Schmidt, D.G. Bogard, Film cooling with compound angle holes: heat transfer, ASME J. Turbomachinery 118 (1996) 800–806.
[5] K. Thole, M. Gritsch, A. Schulz, S. Wittig, Flowfield measurements for film-cooling holes with expanded exits, ASME J. Turbomachinery 120 (1998) 327–336.
[6] E.L. McGrath, J.H. Leylek, Physics of hot crossflow ingestion in film cooling, ASME Paper No. 98-GT-191, 1998.
[7] H.H. Cho, D.H. Rhee, B.G. Kim, Film cooling effectiveness and heat/mass transfer coefficient measurement around a conical-shaped hole with a compound angle injection, ASME Paper No. 99-GT-38, 1999.
[8] H. Reiss, A. Bölcs, Experimental study of showerhead cooling on a cylinder comparing several configurations using cylindrical and shaped holes, ASME J. Turbomachinery 122 (2000) 161–169.
[9] A. Kohli, D.G. Bogard, Effects of hole shape on film cooling with large angle injection, ASME Paper No. 99-GT-165, 1999.
[10] W.H. Echols, J.A. Young, Studies of portable air-operated aerosol generators, NRL Report 5929, 1963.
[11] D.J. Farina, J.M. Hacker, R.J. Moffat, J.K. Eaton, Illuminant invariant calibration of thermochromic liquid crystals, Exp. Therm. Fluid Sci. 9 (1994) 1–12.
[12] C. Camci, K. Kim, S.A. Hippensteele, A new hue capturing technique for the quantitative interpretation of liquid crystal images used in convective heat transfer studies, ASME J. Turbomachinery 114 (1992) 765–775.
[13] J.L. Hay, D.K. Hollingsworth, Calibration of micro-encapsulated liquid crystals using hue angle and a dimensionless temperature, Exp. Therm. Fluid Sci. 18 (1998) 251–257.
[14] S.J. Kline, F.A. McClintock, Describing uncertainties in single sample experiments, Mech. Eng. 75 (1953) 3–8.

[15] I.S. Jung, J.S. Lee, Effects of orientation angles on film cooling over a flat plate: boundary layer temperature distributions and adiabatic film cooling effectiveness, ASME J. Turbomachinery 122 (2000) 153–160.

[16] R.J. Goldstein, P. Jin, R.L. Olson, Film cooling effectiveness and mass/heat transfer coefficient downstream of one row of discrete holes, ASME J. Turbomachinery 121 (1999) 225–232.